SHEAR BEHAVIOUR ANALYSIS OF REINFORCED CONCRETE BEAM USING NON-LINEAR FINITE ELEMENT SIMULATION

Rahmat D. Sutrisno[a*], Harun Alrasyid[a], Wahyuniarsih Sutrisno[a]

Abstract: *This paper investigates shear behaviour of reinforced concrete using multi-surface plasticity model. This analysis uses nonlinear finite element simulation using 3D-NLFEA finite element package. The experimental data adopted from the results of experimental test on eighteen beams where nine beams carried out by Bresler and Scordelis in 1963 and similar nine beams carried out by Vecchio and Shim in 2004. The constitutive model for the concrete material which used in this simulation is based on the plasticity-fracture model and considered the tension stiffening effect for the concrete. The result of the numerical simulation latter compared with the experimental test including load-deflection response, cracking pattern, and failure mode. Based on the analysis result, it was found that the load-deflection response shows slightly higher. For Bresler and Scordelis beams test, the mean ratio of prediction peak load to actual peak load from the experimental result and a coefficient of variation of 1.00 and 7.42%, respectively and for Vecchio and Shim beams test, the mean ratio of prediction peak load to actual peak load from the experimental result and a coefficient of variation of 0.92 and 4.04%, respectively. However, the cracking pattern and failure mode of the beam shows good result which is in compliance with the experimental test.*

Keywords: *Shear failure, plasticity-fracture model, nonlinear finite element, 3D-NLFEA*

INTRODUCTION

Predicting shear failure in beam reinforced concrete is still challenging in non-linear finite element analysis. The proper concrete constitutive model is one of main factors which can affect the prediction of the shear behaviour of reinforced concrete beams. The shear capacity of the reinforced concrete beam depends on the combination of the concrete shear strength and the configuration of the shear reinforcement. Previous study by [1] tested 24 beam specimens with a combination of tensile and shear loads. Based on the tests that have been carried out, it was found that the decrease in shear capacity of concrete beam is affected by the amount and distribution of longitudinal reinforcement. Specimen with adequate amount of longitudinal reinforcement, has more reduction of shear capacity than the specimen without enough longitudinal reinforcement.

The response of reinforced concrete beam can be admitted as linear under normal conditions [2], the result can turn out to be non-linear when reinforced concrete beams are given a very extreme load such as seismic event [3]. Non-linear response can also occur when the applied load is greater than the capacity of the reinforced concrete beam such as, poor design or construction [4-7] so that the influence of concrete and steel reinforcement greatly affects the non-linear response of these elements. For concrete, the non-linear response causes complex concrete cracking behaviour, where in general the concrete will exhibit crack formation and opening/closing of pre-existing cracks, crack slip and shear transfer along the crack interface and crack-to-crack interactions [8-11].

For steel reinforcement, when compared to concrete, steel reinforcement has more linear material properties. Researchers [2][12][13] say that, in service loads, the stress strain of steel reinforcement can be predicted to occur along the steel reinforcement embedded in the concrete this is due to the presence of cracks in the concrete, the bond conditions between the concrete and the reinforcement and the dowel action, then when the steel reinforcement begins to yield steel reinforcement begins to become a non-linear material and becomes dominant in the overall structural response. This is due to the large deformation caused by the yielding of the steel reinforcement. Although it is very good for design because of the ductile response of steel reinforcement, it can cause more severe damage to concrete so that modelling simulations are needed to be able to know the behaviour of reinforced concrete which is very complex [2]. So that later the results of simulations from modelling can be used for design purposes.

For design purposes, the empirical equation used for estimating the shear capacity of reinforced concrete beam is derived from many experimental tests, which the accuracy is vary significantly. However, the non-linear finite element analysis is a technique which able to predict the shear capacity of reinforced concrete beams with fairly accurate results. In order to get the accurate prediction of peak load and crack pattern associated with concrete shear behaviour the non-linear finite element method and proper concrete constitutive model are necessary.

In this paper, a constitutive model that are based on multi surface plasticity-fracture model [14] is used. The Modified Compression Field Theory (MCFT) model was able to accurately predict the shear behaviour of reinforced concrete beam. Modified Compression Field Theory (MCFT) is theory that used by [15] which can predict shear behaviour accurately. However, the reinforcing bars are modelled as smeared reinforcement rather than embedded formulation which requires further justification to determine the reinforcement ratio. For a complex reinforcement arrangement, it would be not practical to precompute the reinforcement ratio for the input in the modelling.

In this paper, isotropic fracture model is used to investigate the shear behaviour of reinforced concrete beam. The prediction of peak load and crack propagation at some point in the load-deflection curve are presented. The reinforced concrete beams will be model as a whole beam, although some researchers perform simulation with half the beam for symmetrical beams but the cracks that occur can be different between the right and left sides.

[a]Civil Engineering Department, Institut Teknologi Sepuluh Nopember, ITS Campus, Sukolilo, Surabaya 60111, Indonesia. Corresponding author email address: rahmatdwisutrisno@gmail.com

RESEACRH SIGNIFICANCE

The research presents shear behaviour of reinforced concrete beam, which will contain peak load and displacement curves, as well as crack patterns that occur in reinforced concrete beams using an in-house 3D-NLFEA finite element package. The material and geometry of the reinforced concrete beam specimens used, were taken from experimental test performed by Bresler and Scordelis as well as Vecchio and Shim [16].

METHODOLOGY

The 3D-NLFEA, which is finite element package developed by [14][17], was used in this research to simulate the shear behaviour of reinforced concrete beam. This package use SALOME and PARAVIEW as pre and post-processor, respectively [18]. The Piscesa et al plasticity-fracture constitutive model [17][19][20] was used in this package and it has been developed by adopting several constitutive model from previous researcher such as [21] and [22] where for the failure surface, Piscesa et. al. [19] use the modified failure surface model from [21] by modifying the parameter which often used to adjust the peak and residual stress for specific concrete strength, which is known as the frictional driver parameters, based on the equation from [22][23].

The fracture energy used for reinforced concrete beam are computed using the CEB-FIP 1990 [24] with the maximum aggregate size was set to 25 mm. The input for the base fracture energy (GF_0) is 0.03 N/mm where the base tensile fracture energy (GF_0) is a function of the maximum aggregate diameter and is scaled by concrete compressive strength. For the tension stiffening that will be used in the modelling in this paper, the equation used is based on [15]. According to [25] the tension stiffening effect is defined as the ability of the intact concrete between the cracks to withstand part of the tensile forces or the contribution of the intact concrete between the cracks to the stiffness of the structural element. The tension stiffening in the plasticity fracture model can be computed using Equation 1:

$$f_{c1} = \frac{f_{cr}}{1+\sqrt{200\varepsilon_1}} \quad (1)$$

Where f_{c1} is the concrete principal tensile stress, ε_1 is principal tensile strain in concrete and f_{cr} is the stress in concrete at cracking. In this model the tension stiffening is applied directly to entire meshes of concrete because it affect the input stress strain diagram of concrete During the pre-processor stages, the maximum mesh size of the hexahedral element is set to 25 mm, because it adjusts to a predetermined size of maximum aggregate. Hence, theoretically, the internal length scale should be set to 25 mm for reinforced concrete beams.

The constitutive model for the steel reinforcing bar is modelled using an elastic-perfectly plastic model which the material model with the first line as the initial elastic section has the value of the modulus of elasticity of steel, Es. The second line represents the plasticity of the steel by hardening and the slope is the hardening modulus, E_{sh}. In terms of perfect plasticity where $E_{sh} = 0$. The limiting strain L indicates the limited ductility of the steel [26].

In this paper, there are eighteen beams are investigated based on the experimental test performed by Bresler and Scordelis as well as Vecchio and Shim [16]. Based on research conducted by Vecchio and Shim, there are 12 beams each, of which 3 beams are without stirrups and 9 beams are with stirrups. The modelling of the beam without stirrups has been previously modelled by [27] so that in this paper the modelling will be focused on beams that use stirrups reinforcement.

All beams were rectangular cross section and consist of three series of beam which differed by the amount of longitudinal and shear reinforcement, cross sectional dimensions, span length, and strength of concrete materials. The cross-section details and material properties of Bresler-Scodelis and Vecchio-Shim beam showed in Table 1 and Table 2. In order to easily identify the sample, the code was applied, which is BS code shows the beam tested by Bresler-Scodelis and VS code shows the beam tested by Vecchio-Shim.

In term of longitudinal reinforcement, the BS beam has same top reinforcement, which is two of No.4 reinforcement. However, in term of longitudinal reinforcement, the number of reinforcements is varying from two to six No. 9 reinforcement. Based on the [16], the VS beam use a metric sized bar was used instead the imperial size bar due to unviability of adequate amounts of imperial size bar. For VS beam, the top longitudinal reinforcement uses 3M10 and the bottom reinforcement use combination of M30 and M25 steel reinforcement. For the stirrups, the BS beams use No. 2 bar, while the VS use D5 bar instead. The detail of dimension and area of metric and imperial bar use in this paper shown in Table 1.

Table 1 Material properties, (a) Bresler-Scodelis beams, (b) Vecchio-Shim beams [16]

No	Bar Size	Diameter	Area	f_y	f_u	E_s
		mm	mm^2	MPa	MPa	MPa
1	M10	11.3	100	315	460	200000
2	M25	25	500	445	680	220000
3	M30	30	700	436	700	200000
4	D4	3.7	25.7	600	651	200000
5	D5	6.4	32.2	600	651	200000

(a)

No	Bar Size	Diameter	Area	f_y	f_u	E_s
		mm	mm^2	MPa	MPa	MPa
1	No.2	6.4	32.2	325	430	190000
2	No.4	12.7	127	345	542	201000
3	No.9	28.7	645	555	933	218000

(b)

The concrete is assumed to have a compressive strength of 0.85f'c where 0.85 is a factor to reduce the actual concrete strength of the beam to consider the different strength between concrete beam and the cylinder, which can affect by the dimension and curing condition of the specimens. The ACI 318-19 was used to calculate the modulus elasticity for the concrete material. The concrete tensile strength (ft) used as an input is taken about 80% from the estimated concrete tensile strength without silica fume as outlined in [22], [23].

The modelling consideration for beams which will be modelled in 3D-NLFEA using eight-node hexahedral solid element and for the rebar element was modelled using wire element. Bonding for solid element and wire element was

Table 2 Cross section detail and concrete properties of Bresler-Scodelis beams and Vecchio-Shim beams [16]

No	Beam Number	b mm	h mm	d mm	L mm	Span mm	Bottom Steel	Top Steel	Stirrups	f'_c MPa
1	BS-A1	307	561	466	4100	3660	4 No. 9	2 No. 4	No. 2-210	24.1
2	BS-A2	305	559	464	5010	4570	5 No. 9	2 No. 4	No. 2-210	24.3
3	BS-A3	307	561	466	6840	6400	6 No. 9	2 No. 4	No. 2-210	35.1
4	BS-B1	231	556	461	4100	3660	4 No. 9	2 No. 4	No. 2-190	24.8
5	BS-B2	229	561	466	5010	4570	4 No. 9	2 No. 4	No. 2-190	23.2
6	BS-B3	229	556	461	6840	6400	5 No. 9	2 No. 4	No. 2-190	38.8
7	BS-C1	155	559	464	4100	3660	2 No. 9	2 No. 4	No. 2-210	29.6
8	BS-C2	152	559	464	5010	4570	4 No. 9	2 No. 4	No. 2-210	23.8
9	BS-C3	155	554	459	6840	6400	4 No. 9	2 No. 4	No. 2-210	35.1
10	VS-A1	305	552	457	4100	3660	2 M30, 2 M25	3 M10	D5-210	22.6
11	VS-A2	305	552	457	5010	4570	3 M30, 2 M25	3 M10	D5-210	25.9
12	VS-A3	305	552	457	6840	6400	4 M30, 2 M25	3 M10	D4-168	43.5
13	VS-B1	229	552	457	4100	3660	2 M30, 2 M25	3 M10	D5-190	22.6
14	VS-B2	229	552	457	5010	4570	2 M30, 2 M25	3 M10	D5-190	25.9
15	VS-B3	229	552	457	6840	6400	3 M30, 2 M25	3 M10	D4-152	43.5
16	VS-C1	152	552	457	4100	3660	2 M30	3 M10	D5-210	22.6
17	VS-C2	152	552	457	5010	4570	2 M30, 2 M25	3 M10	D5-210	25.9
18	VS-C3	152	552	457	6840	6400	2 M30, 2 M25	3 M10	D4-168	43.5

Table 3 Comparison of experimental result versus VecTor2 and 3D-NLFEA

Beam	Ultimate Load (kN)					Midspan Deflection (mm)				
	Pu Test	Pu VecTor 2	Pu 3D-NLFEA	Pu test/Pu VecTor2	Pu Test/Pu 3D-NLFEA	Displ Test	Displ VecTor 2	Displ 3D-NLFEA	Displ test/Displ VecTor2	Displ Test/Displ 3D-NLFEA
BS-A1	468	472	528	0.99	0.89	14.2	15.8	21.4	0.9	0.66
BS-A2	490	399	502	1.23	0.98	22.9	19.5	29.2	1.17	0.78
BS-A3	468	366	448	1.28	1.05	35.8	44.6	43.8	0.8	0.82
BS-B1	446	423	483	1.06	0.92	13.7	15.3	22.2	0.9	0.62
BS-B2	400	327	382	1.22	1.05	20.8	19.5	27.2	1.07	0.76
BS-B3	356	355	359	1.00	0.99	35.3	39	43.2	0.91	0.82
BS-C1	312	307	273	1.02	1.14	17.8	18.3	20	0.97	0.89
BS-C2	324	258	323	1.26	1.00	20.1	17.3	26	1.16	0.77
BS-C3	270	255	266	1.06	1.02	36.8	36.3	40.9	1.01	0.90
		Mean		1.12	1.00		Mean		0.99	0.78
		COV (%)		10.69	7.42		COV (%)		12.76	11.95
Beam	Pu Test	Pu VecTor 2	Pu 3D-NLFEA	Pu test/Pu VecTor2	Pu Test/Pu 3D-NLFEA	Displ Test	Displ VecTor 2	Displ 3D-NLFEA	Displ test/Displ VecTor2	Displ Test/Displ 3D-NLFEA
VS-A1	459	476	520	0.96	0.88	18.8	14.3	23.6	1.31	0.80
VS-A2	439	457	507	0.96	0.87	29.1	21.8	28.8	1.33	1.01
VS-A3	420	447	457	0.94	0.92	51	51.3	47.2	0.99	1.08
VS-B1	434	423	477	1.03	0.91	22	15.8	23.1	1.39	0.95
VS-B2	365	384	392	0.95	0.93	31.6	22.3	27.4	1.42	1.15
VS-B3	342	376	366	0.91	0.93	59.6	51.2	42.6	1.16	1.40
VS-C1	282	289	288	0.98	0.98	21	15.3	21.6	1.37	0.97
VS-C2	290	306	322	0.95	0.90	25.7	20.6	28.4	1.25	0.90
VS-C3	265	283	273	0.94	0.97	44.3	43.2	37.6	1.03	1.18
		Mean		0.96	0.92		Mean		1.25	1.05
		COV (%)		3.45	4.04		COV (%)		12.55	16.92
Total		Mean		1.04	0.96		Mean		1.12	0.92
		COV (%)		11.63	7.39		COV (%)		17.25	21.32

modelled using tie constraint type and the boundary condition, which will define the bearings and loads in the model, used three point bending scheme and displacement control loading techniques according to the experimental test conducted by [16]. Figure 1 shows the how the beams model is tested. The loading is given with a displacement control of -0.1 mm for every load step.

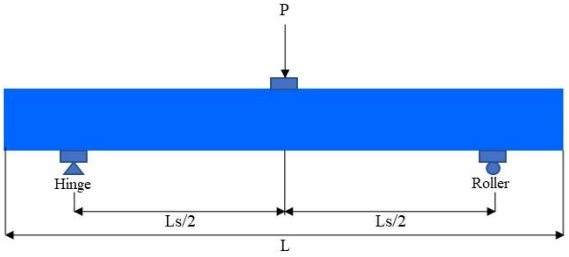

Figure 1 Beam Test Scheme [16]

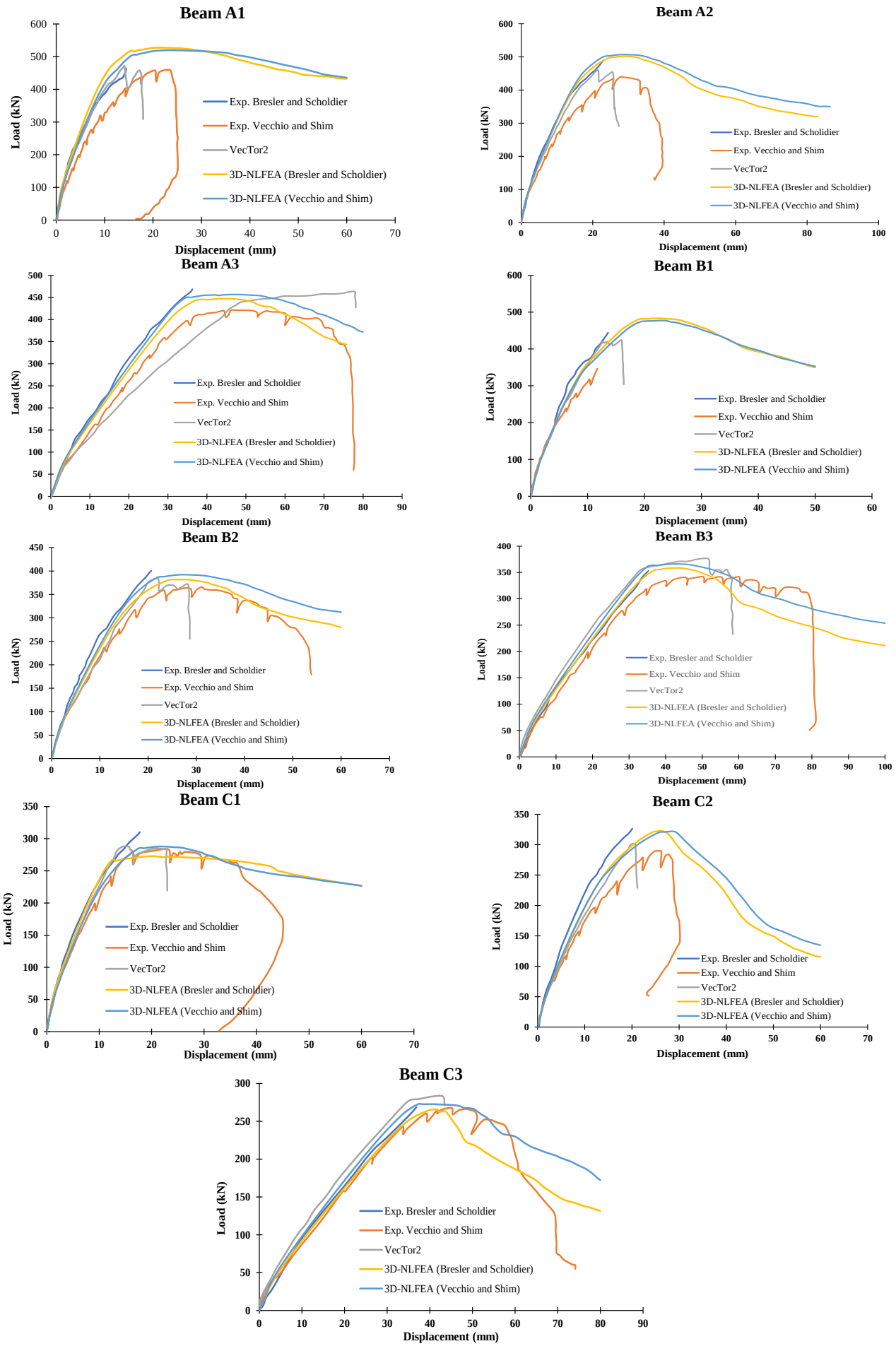

Figure 2 Load deflection curve for Bresler-Scordelis and the Vecchio-Shim beams

ANALYSIS AND DISCUSSION

A. LOAD-DEFLECTION COMPARISON

This section shows the load-deflection output based on the modelling result of 18 beams. Figure 2 show the load-deflection curve for eighteen beams. As for the numerical simulation, in addition to the 3D-NLFEA results, numerical simulation results from VecTor 2 which utilize the MCFT approach were also shown in Figure 2. As shown in Figure 2 beam A1, A2 and B1 shows higher peak load and displacement compared to the beam tested by Bresler and Scordelis and Vecchio and Shim [16]. This could be caused by the addition of a tension stiffening effect which according to [25] the tension stiffening effect is expressed as the contribution of the intact concrete between the cracks to the stiffness of the structural elements or the ability of the intact concrete between the cracks to withstand some of the resulting tensile forces. In this model, the tension stiffening effect was considered and resulting increase of shear and flexural strength of the reinforced concrete beam. The contribution of the cracked concrete also increases the non-linear stiffness of the beam under stress. All those effects were combined and finally cause increase in the displacement and peak load of the beam [25].

On the other hand, the concrete material properties can vary significantly. Researcher [27] express the aggregate size and composition may affect the fracture energy, initial micro-cracks, and the strength of the concrete material.

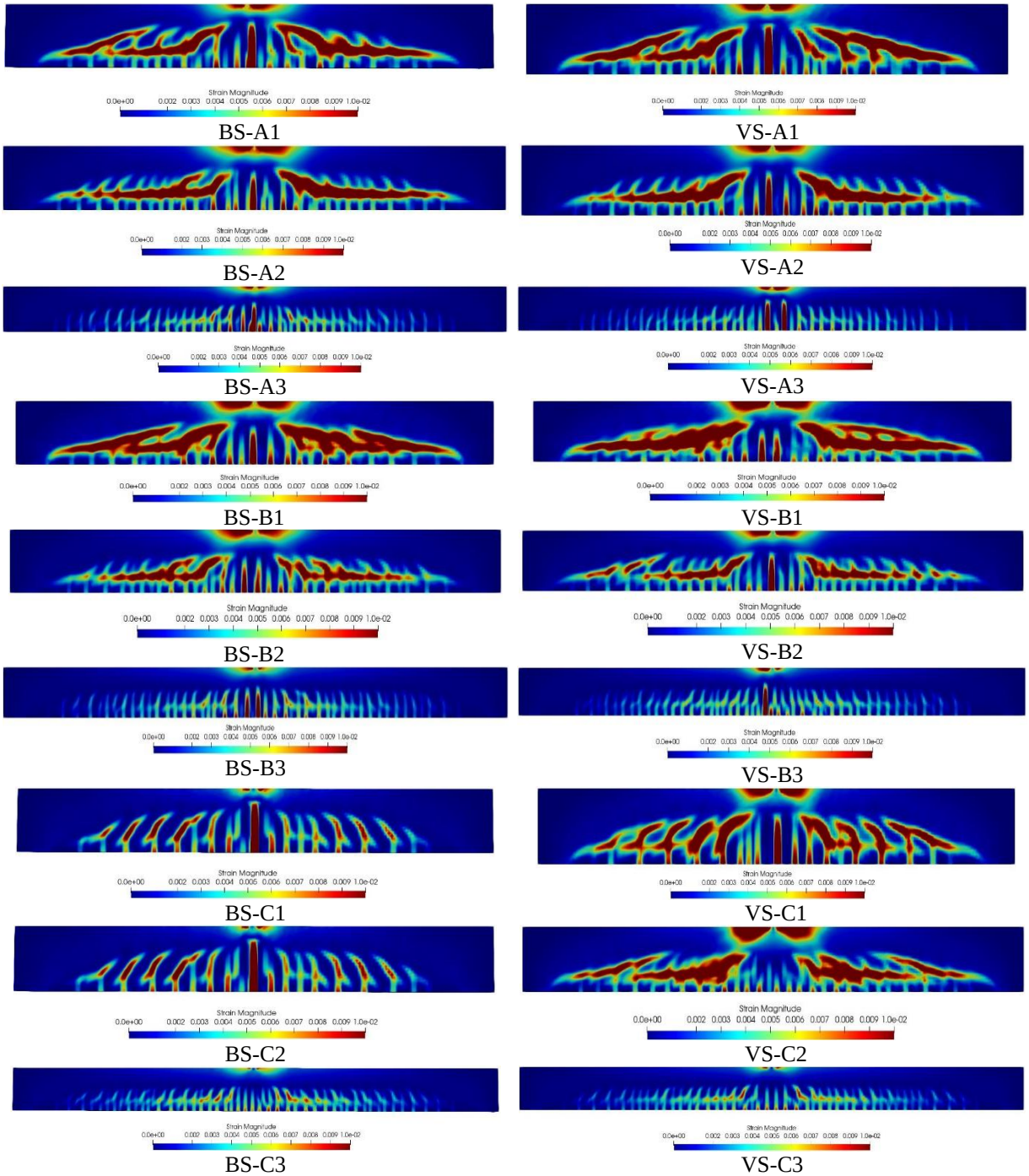

Figure 3 Crack pattern comparison for Bresler-Scordelis and the Vecchio-Shim beams

Different curing condition and loading parameter may also affect the behaviour of the tested beam. As for the different in numerical results, 3D-NLFEA utilize different concrete constitutive models which incorporates plasticity-fracture model with isotropic fracture formulation and embedded rebar formulation, therefore author thought that for the 3D-NLFEA results, despite of different measurement equipment accuracy, the concrete compressive strength, tensile strength, fracture energy and tension stiffening effect were one of the causes of the significant difference in the load-deflection curve.

The ultimate strengths calculated from the 3D-NLFEA are compared to experimental results and VecTor2 results for both the Vecchio-Shim and Bresler-Scordelis. Table 3 are the calculated load–deflection responses for the both the Bresler-Scordelis and the Vecchio-Shim beams. Based on the result as shown in Table 3, the result shows a reasonably accurate simulations of strength and load deformation response. For the combined set of 9 beams on Bresler-Scordelis beams, the ratio of the experiment to 3D-NLFEA strength (Pu Test /Pu 3D-NLFEA) had a mean of 1.00 and a coefficient of variation of 7.42%. That result was better than the ratio of the experiment to VecTor2 strength (Pu Test /Pu VecTor2) which had a mean of 1.12 and a coefficient of variation of 10.69%, so that for Bresler-Scordelis beams 3DNLFEA is able to predict strength better than VecTor2. For the combined set of 9 beams on Vecchio-Shim beams, the ratio of the experiment to 3D-NLFEA strength (Pu Test /Pu 3D-NLFEA) had a mean of 0.92 and a coefficient of variation of 4.04%. That result was overestimated than the ratio of the experiment to VecTor2 strength (Pu Test /Pu VecTor2) which had a mean of 0.96 and a coefficient of variation of 3.45% but that result is still acceptable because the different between ratio of the experiment to 3D-NLFEA strength (Pu Test /Pu 3D-NLFEA) and ratio of the experiment to VecTor2 strength (Pu Test /Pu VecTor2) is not that much.

On the other hand, the combined set of 18 beams, the ratio of the experiment to 3D-NLFEA strength (Pu Test /Pu 3D-NLFEA) had a mean of 0.96 and a coefficient of variation of 7.39%. When compared to combined set of 18 beams, the ratio of the experiment to VecTor2 strength (Pu Test /Pu VecTor2) had a mean of 1.04 and a coefficient of variation of 11.63%, the ratio of the experiment-to 3D-NLFEA strength were slightly overestimated. Where, as previously explained that for the 3D-NLFEA results, despite of different measurement equipment accuracy, the concrete compressive strength, tensile strength, fracture energy and tension stiffening effect were one of the causes of the significant difference in the load-deflection curve but, the difference ratio and coefficient of variation of the experiment to 3D-NLFEA strength (Pu Test /Pu 3D-NLFEA) and the experiment to VecTor2 strength (Pu Test /Pu VecTor2) are still acceptable.

B. CRACK PATTERN COMPARISON

Figure 3 shows the crack pattern for eighteen beams, the maximum strains at maximum displacement points in the load-deflection curve is investigated. As shown in Figure 3 beam A1, A2, B1, B2, C1, and C2 the failure mode of the beams can be described as shear compression and for beam A3, B3 and C3 the failure mode of the beams can describe as flexural compression. Compared with the experimental result conducted by previous researchers[16], [28], it shows that the crack pattern as the modelling results of 3DNLFEA were similar with both experimental tests performed by Vecchio-Shim and Bresler-Scordelis. The beam A1, A2, B1, B2, C1, and C2 has short and intermediate span beam with the shear-compression failure mode and the diagonal cracks were formed at approximately 60% of the ultimate load which is in accordance with the experiment performed by Bresler-Scordelis [28].

After the diagonal tension cracks occurred, the additional load cause further diagonal cracking and finally, the final failure of the beam occurred at the compression zone. For beam A3, B3 and C3 it has long span, and the failure mode was flexure-compression. This crack pattern is in accordance with the experimental test performed by Vecchio-Shim and Bresler-Scordelis [28]. Due to large span length of the beam, the cracks in this type of beam were dominated by flexural cracks. As additional load applied, the number of cracks was increased, but the diagonal tension cracks never developed into major critical cracks while flexural cracks continued to extend upward. Vecchio et al, [16] expressed that shear-compression failure mode was dominant in the intermediate-span beams and flexure compression mode prevailed in the long span beams. Based on the modelling result, it can be conclude that the crack pattern of all 18-beams were in accordance with the experiments [16], [28] that have been carried out previously.

CONCLUSIONS

This paper has presented nonlinear finite element simulation of reinforced concrete. Plasticity fracture model and tension stiffening effect was use for the concrete constitutive model. 3D-NLFEA software package was used in the numerical simulation to utilize full three-dimensional model of the beam and random imperfection material to get result for nonlinear finite element simulation. Based on the work presented, plasticity fracture model and tension stiffening effect can provide acceptable predictions of load and deflection capacities. A mean peak load of experimental to 3D-NLFEA (Pu Test /Pu 3D-NLFEA) had mean of 0.96 and a coefficient of variation of 7.39%. It shown that a little bit overestimated then mean peak load of experimental to VecTor2 (Pu Test /Pu VecTor2) result which had a mean of 1.04 and a coefficient of variation of 11.63%. For crack pattern comparison the result from 3D-NLFEA show that for beam with short and intermediate span the failure can be describe as shear compression and for beam with long span the failure can be describe as flexural compression. The result from 3D-NLFEA has the same as experimental result which for shear compression mode was dominant in the intermediate-span beams and flexure compression mode prevailed in the long span beams.

This show that 3D-NLFEA software package can produce result that are close to the experimental results, so that can help engineers not only to assess the response of structural elements in detail but also to predicting response of structural elements in detail. The post-processing in 3D-NLFEA can be very helpful in the process of predicting a

structural element as well as assessing the ability of a structural element.

REFERENCES

[1] S. B. and M. P. C. Bhide, "Influence of axial tension on the shear strength of transversally reinforced concrete beams," *ACI Structural Journal*, vol. 86, no. 5, pp. 570–581, 1989, doi: 10.1002/suco.202000278.

[2] A. Tambusay, P. Suprobo, B. Suryanto, and W. Don, "Application of nonlinear finite element analysis on shear-critical reinforced concrete beams," *Journal of Engineering and Technological Sciences*, vol. 53, no. 4, 2021, doi: 10.5614/j.eng.technol.sci.2021.53.4.8.

[3] B. I. Bae, J. H. Chung, H. K. Choi, H. S. Jung, and C. S. Choi, "Experimental study on the cyclic behavior of steel fiber reinforced high strength concrete columns and evaluation of shear strength," *Engineering Structures*, vol. 157, December 2017, pp. 250–267, 2018, doi: 10.1016/j.engstruct.2017.11.072.

[4] A. Sharma, R. Eligehausen, and J. Hofmann, "Seismic assesment of poorly designed rc frame structures seismic assesment of poorly designed RC frame structures considering joint," *Conference: 4th International FIB Congress*, November, 2014, doi: 10.13140/2.1.2516.9608.

[5] K. V. Duong, S. A. Sheikh, and F. J. Vecchio, "Seismic behavior of shear-critical reinforced concrete frame: Experimental investigation," *ACI Structural Journal*, vol. 104, no. 3, pp. 304–313, 2007, doi: 10.14359/18620.

[6] M. M. Ziara, D. Haldane, and S. Hood, "Proposed changes to flexural design in BS 8110 to allow over-reinforced sections to fail in a ductile manner," *Magazine of Concrete Research*, vol. 52, no. 6, pp. 443–454, 2000, doi: 10.1680/macr.2000.52.6.443.

[7] M. P. Collins, E. C. Bentz, E. G. Sherwood, and J. K. Wight, "Where is shear reinforcement required? review of research results and design procedures.," *ACI Structural Journal*, vol. 106, no. 4, p. 556, 2009.

[8] A. Pimanmas and K. Maekawa, "Finite element analysis and behaviour of pre-cracked reinforced concrete members in shear," *Magazine of Concrete Research*, vol. 53, no. 4, pp. 263–282, 2001, doi: 10.1680/macr.53.4.263.51365.

[9] B. Bujadham and K. Maekawa, "the Universal Model for Stress Transfer Across Cracks in Concrete," *Doboku Gakkai Ronbunshu*, vol. 1992, no. 451, pp. 277–287, 1992, doi: 10.2208/jscej.1992.451_277.

[10] B. Suryanto, K. Nagai, and K. Maekawa, "Modeling and analysis of shear-critical ECC members with anisotropic stress and strain fields," *Journal of Advanced Concrete Technology*, vol. 8, no. 2, pp. 239–258, 2010, doi: 10.3151/jact.8.239.

[11] B. Suryanto, K. Nagai, and K. Maekawa, "Smeared-crack modeling of R/ECC membranes incorporating an explicit shear transfer model," *Journal of Advanced Concrete Technology*, vol. 8, no. 3, pp. 315–326, 2010, doi: 10.3151/jact.8.315.

[12] A. Belarbi and T. T. C. Hsu, "Constitutive laws of concrete in tension and reinforcing bars stiffened by concrete," *ACI Structural Journal*, vol. 91, no. 4, pp. 465–474, 1994, doi: 10.14359/4154.

[13] H. Shima, L. L. Chou, and H. Okamura, "Micro and macro models for bond in reinforced concrete.," *Journal of the Faculty of Engineering, University of Tokyo, Series B*, vol. 39, no. 2. pp. 133–194, 1987.

[14] B. Piscesa, M. M. Attard, D. Prasetya, and A. K. Samani, "Modeling cover spalling behavior in high strength reinforced concrete columns using a plasticity-fracture model," *Engineering Structures*, vol. 196, June, p. 109336, 2019, doi: 10.1016/j.engstruct.2019.109336.

[15] F. J. Vecchio and M. P. Collins, "Modified compression-field theory for reinforced concrete elements subjected to shear," *Journal of the American Concrete Institute*, vol. 83, no. 2. pp. 219–231, 1986, doi: 10.14359/10416.

[16] F. J. and S. W. Vecchio, "Experimental and analytical reexamination of classic concrete beam tests," *Journal of Structural Engineering*, vol. 9445, April 2004, pp. 1562–1569, 2004, doi: 10.1061/(ASCE)0733-9445(2004)130.

[17] B. Piscesa, M. M. Attard, and A. K. Samani, "3D finite element modeling of circular reinforced concrete columns confined with FRP using a plasticity based formulation," *Composite Structures*, vol. 194, pp. 478–493, 2018, doi: 10.1016/j.compstruct.2018.04.039.

[18] U. Ayachit, *The paraview guide: a parallel visualization application*, United States: Kitware Inc. 2015.

[19] B. Piscesa, M. M. Attard, A. K. Samani, and S. Tangaramvong, "Plasticity constitutive model for stress-strain relationship of confined concrete," *ACI Materials Journal*, vol. 114, no. 2, pp. 361–371, 2017, doi: 10.14359/51689428.

[20] B. Piscesa, M. M. Attard, and A. K. Samani, "A lateral strain plasticity model for FRP confined concrete," *Composite Structures*, vol. 158, pp. 160–174, 2016, doi: 10.1016/j.compstruct.2016.09.028.

[21] P. Menetrey and K. J. Willam, "Triaxial failure criterion for concrete and its generalization," *ACI Structural Journal*, no. 92, pp. 311–318, 1996.

[22] M. M. Attard and S. Setunge, "Stress-strain relationship of confined and unconfined concrete," *ACI Materials Journal*, vol. 93, no. 5, pp. 432–442, 1996, doi: 10.14359/9847.

[23] A. K. Samani and M. M. Attard, "A stress-strain model for uniaxial and confined concrete under compression," *Engineering Structures*, vol. 41, pp. 335–349, 2012, doi: 10.1016/j.engstruct.2012.03.027.

[24] C. E. I. D. Beton, *CEB FIP model code 1990*, London: Thomas Telford Ltd., 1993.

[25] M. P. Martins, C. S. Rangel, M. Amario, J. M. F. Lima, P. R. L. Lima, and R. D. Toledo Filho, "Modelling of tension stiffening effect in reinforced recycled concrete," *Revista Instituto Brasileiro do Concreto de Estruturas e Materiais*, vol. 13, no. 6, pp. 1–21, 2020, doi: 10.1590/s1983-41952020000600005.

[26] V. Červenka and J. Červenka, *ATENA theory updated*, Prague: Cervenka Consulting Ltd., 2018.

[27] B. Piscesa, H. Alrasyid, D. Prasetya, and D. Iranata, "Numerical investigation of reinforced concrete beam due to shear failure," *IPTEK The Journal for Technology and Science*, vol. 31, no. 3, p. 373, 2021, doi: 10.12962/j20882033.v31i3.7385.

[28] B. Bhide. and A. C. Scordelis, “Shear strength of reinforced concrete beams,” *Journal of American Concrete Institute*, no. 3, pp. 51–74, 1963.